Journal of Power Sources 183 (2008) 724–729

Contents lists available at ScienceDirect

Journal of Power Sources

journal homepage: www.elsevier.com/locate/jpowsour

A rechargeable lithium metal battery operating at intermediate temperatures using molten alkali bis(trifluoromethylsulfonyl)amide mixture as an electrolyte

Atsushi Watarai[a], Keigo Kubota[a], Masaki Yamagata[a], Takuya Goto[a], Toshiyuki Nohira[a], Rika Hagiwara[a,*], Koichi Ui[b], Naoaki Kumagai[b]

[a] Department of Fundamental Energy Science, Graduate School of Energy Science, Kyoto University, Sakyo-ku, Kyoto 606-8501, Japan
[b] Department of Frontier Materials and Functional Engineering, Graduate School of Engineering, Iwate University, 4-3-5 Ueda, Morioka, Iwate 020-8551, Japan

ARTICLE INFO

Article history:
Received 23 April 2008
Received in revised form 20 May 2008
Accepted 21 May 2008
Available online 27 May 2008

Keywords:
Lithium battery
Molten salt
Ionic liquid
Bis(trifluoromethylsulfonyl)amide
$LiFePO_4$
Olivine

ABSTRACT

The physicochemical properties of molten alkali bis(trifluoromethylsulfonyl)amide, MTFSI (M = Li, K, Cs), mixture (x_{LiTFSI} = 0.20, x_{KTFSI} = 0.10, x_{CsTFSI} = 0.70) were studied to develop a new rechargeable lithium battery operating at intermediate temperature (100–180 °C). The viscosity and ionic conductivity of this melt at 150 °C are 87.2 cP and 14.2 mS cm^{-1}, respectively. The cyclic voltammetry revealed that the electrochemical window at 150 °C is as wide as 5.0 V, and that the electrochemical deposition/dissolution of lithium metal occurs at the cathode limit. A Li/MTFSI (M = Li, K, Cs)/$LiFePO_4$ cell showed an excellent cycle performance at a constant current rate of C/10 at 150 °C; 95% of the initial discharge capacity was maintained after 50 cycles. Except for the initial few cycles, the coulombic efficiencies were approximately 100% for all the cycles, indicating the stabilities of the molten MTFSI mixture and all the electrode materials.
© 2008 Elsevier B.V. All rights reserved.

1. Introduction

Rechargeable lithium batteries have been widely used as high performance power sources for portable electronic devices owing to their high energy densities and cycleabilities. In recent years, the rechargeable lithium batteries have also been highly expected to be used for electric vehicles (EVs), hybrid electric vehicles (HEVs) and storage of surplus electricity [1,2]. However, the current rechargeable lithium batteries have safety problems as symbolized by the recent ignition accidents of laptop computers and mobile phones. When it comes to the large-sized applications as described above, there is quite a possibility that an ignition accident causes terrible disaster. One of the key technologies to improve the safety of the batteries is the development of nonvolatile and nonflammable electrolytes. Rechargeable lithium batteries using room temperature molten salts (RTMSs), often called room temperature ionic liquids (RTILs), recently, as their electrolytes [3,4] have been studied as well as all solid-state lithium batteries [5] from such a viewpoint. However, the operations of these batteries have so far been limited to around room temperature. Considering the large-sized applications, the working temperature is not necessarily limited to room temperature. Conversely, the operation at elevated temperatures is advantageous giving higher ionic conductivity, faster electrode reactions, and thereby high power density that is one of the problems for current rechargeable lithium batteries. Nevertheless, too high temperatures (>180 °C) bring other problems such as difficulty in handling of liquid lithium metal (mp 180.5 °C), requirement of special heating and insulating system, expensive structural materials, etc. Thus, the practical operation temperature of lithium metal rechargeable batteries for the large-sized applications is advantageously extended to intermediate temperatures, 100–180 °C.

Generally, molten salts, or ionic liquids, provide negligibly small volatility, nonflammability, high thermal and electrochemical stabilities. Therefore, they have been studied and used as electrolytes in many electrochemical fields [6–8]. We have recently found that salts consisting of alkali metal cations and bis(trifluoromethylsulfonyl)amide (TFSI) anion, MTFSIs (M = Li, Na, K, Rb, Cs), have melting points at 120–260 °C and their melting points drastically decrease by mixing two or three of them [9,10]. It has also been found that the molten MTFSI mixtures have wide electrochemical windows of approximately 5 V owing to the high electrochemical stability of TFSI anion [11]. Thus, these molten salt mixtures are attractive as electrolytes for many electrochemical applications including rechargeable lithium batteries. According to

* Corresponding author. Tel.: +81 75 753 5822; fax: +81 75 753 5906.
E-mail address: hagiwara@energy.kyoto-u.ac.jp (R. Hagiwara).

0378-7753/$ – see front matter © 2008 Elsevier B.V. All rights reserved.
doi:10.1016/j.jpowsour.2008.05.054

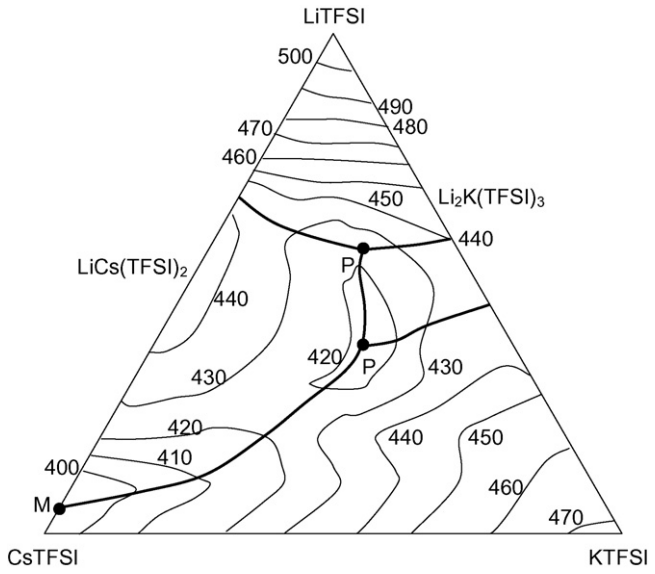

Fig. 1. The phase diagram of (Li, K, Cs)TFSI system given in absolute temperature. P: peritectic point, M: the lowest melting point in the system [10].

our previous studies [9,10], the mixture of (Li, Cs)TFSI (x_{LiTFSI} = 0.07, x_{CsTFSI} = 0.93) has an eutectic point at 117 °C, which is the lowest melting point in all binary and ternary MTFSI systems containing LiTFSI. However, the low concentration of LiTFSI may cause large diffusion overpotential in the high power density operation. To find the optimized melt composition having a higher LiTFSI concentration, we referred to the phase diagram of ternary (Li, K, Cs)TFSI system shown in Fig. 1 [10]. We selected a composition, x_{LiTFSI} = 0.20, x_{KTFSI} = 0.10, x_{CsTFSI} = 0.70, henceforth abbreviated as Li20–K10–Cs70, since it exhibits a lower melting point than that of binary (Li, Cs)TFSI (x_{LiTFSI} = 0.20, x_{CsTFSI} = 0.80) having the same LiTFSI content.

In the present study, viscosity, ionic conductivity and electrochemical window of the Li20–K10–Cs70 melt were measured at several selected temperatures. Then, the electrochemical behavior of lithium deposition/dissolution and the charge–discharge properties of the Li/Li20–K10–Cs70 melt/$LiFePO_4$ cell were investigated at 150 °C.

2. Experimental

2.1. Preparation of MTFSIs

Bis(trifluoromethylsulfonyl)amide, HTFSI (Morita Chemical Industries, purity >99%), K_2CO_3 (Wako Pure Chemical Industries, purity >99.9%) and Cs_2CO_3 (Sigma–Aldrich, purity >99.9%) were used for the preparations of MTFSI salts. MTFSIs (M = K, Cs) were synthesized by neutralization of HTFSI and M_2CO_3 in ethanol at room temperature and then dried under vacuum for 72 h at the temperatures lower than the melting points of each MTFSI. LiTFSI (Morita Chemical Industries, purity >99%) was used after dried under vacuum for 24 h at 150 °C.

2.2. Viscosity and ionic conductivity measurements

Viscosities of the molten salt were measured by a B-type viscometer (Brookfield Engineering Laboratories, DV-II+ Pro). The temperature of the melt was controlled by an electric furnace equipped with a temperature controller (Brookfield Engineering Laboratories, Thermosel).

Ionic conductivities of the molten salt were measured by electrochemical impedance spectroscopy using a calibrated cell with two platinum disk electrodes and a potentiostat/galvanostat/FRA (Princeton Applied Research, PARSTAT 2273). The cell constant was determined by the standard KCl aqueous solution (0.1 D).

2.3. Electrochemical measurements

Electrochemical measurements were performed in a three-electrode system constructed in a Pyrex beaker cell by means of a potentio/galvanostat (Hokuto Denko, HZ-3000). An electrochemical window of the melt was measured by cyclic voltammetry. A lithium foil (Sigma–Aldrich, purity >99.9%) was used as a reference electrode. To investigate the cathode limit, a nickel plate (ϕ 6 mm, t = 0.1 mm) was used as a working electrode and a glassy carbon rod was used as a counter electrode. To investigate the anode limit, a glassy carbon rod (ϕ 3 mm) and a lithium foil were used, respectively, for a working electrode and a counter electrode. The reversibility of lithium deposition/dissolution was investigated by cyclic voltammetry. In this measurement, lithium foils (~0.5 mm thickness) were used for all the three electrodes. The stability of an aluminum current collector was checked by potentiostatic electrolysis of a plate electrode and cyclic voltammetry of a mesh electrode. Lithium foils were used as both counter and reference electrodes.

A charge–discharge test was carried out with a galvanostatic method using a three-electrode cell. Lithium foils were used as negative and reference electrodes. Carbon-coated olivine, $LiFePO_4$, was prepared by aqueous solution method using sucrose as a carbon source and then calcined at 800 °C for 12 h under Ar/H_2 flow [12]. $LiFePO_4$ thus prepared was well mixed with acetylene black (Wako Pure Chemical Industries, purity >99.99%) and PTFE (Sigma–Aldrich) at a weight ratio of 80/15/5 using a mortar and pestle which was then pressed onto an aluminum mesh current collector at 300 MPa. Cell performance was evaluated from the charge–discharge tests at constant current rate of C/10. All the measurements were conducted in an argon glove box (Miwa MFG, DBO-2LKH-O) with a gas-refining instrument. The cell temperature was controlled by a heater with a temperature controller.

2.4. X-ray diffraction (XRD) and differential scanning calorimetry (DSC) measurements

Identification of the deposit at the cathode limit was performed by means of an X-ray diffractometer (Rigaku, MultiFlex-KB) using Cu Kα radiation. The deposited sample was scraped from the Ni plate in a glove box and then put on a glass holder. This holder was wrapped with a translucent flexible film (Pechiney Plastic Packaging, Parafilm) in order to protect the sample from the reaction with air.

A differential scanning calorimeter (Shimadzu, DSC-60) was also used for the identification of the electrochemically deposited materials. The measurement was conducted using a nickel cell under the continuous flow of dried and deoxygenated argon (Kyoto Teisan K.K., purity 99.995%) at 30 ml min^{-1}.

3. Results and discussion

The viscosities and ionic conductivities of Li20–K10–Cs70 melt are plotted against temperature in Figs. 2 and 3, respectively. For example, the viscosity and ionic conductivity at 150 °C are 87.2 cP and 14.2 mS cm^{-1}, respectively. In the cases of the RTILs in which LiTFSI is dissolved, for comparison, the viscosity

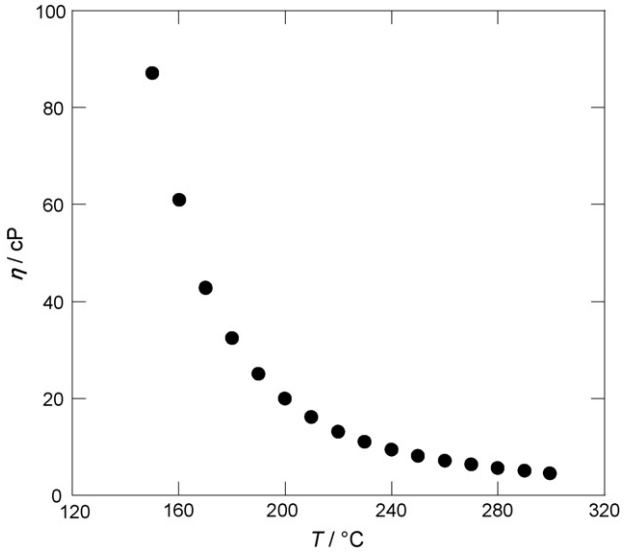

Fig. 2. Temperature dependence of viscosities for Li20–K10–Cs70 melt.

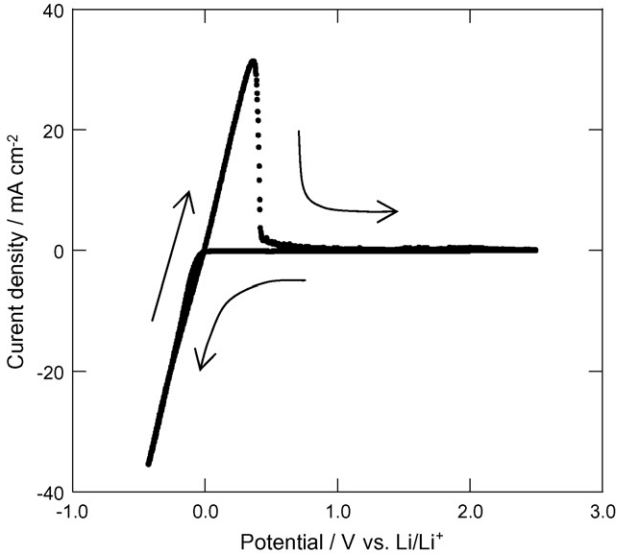

Fig. 4. A cyclic voltammogram of a Ni plate electrode in Li20–K10–Cs70 melt at 150 °C. Scan rate: 10 mV s^{-1}.

and ionic conductivity of 1 M LiTFSI/EMI–TFSI (EMI = 1-ethyl-3-methylimidazolium) are ≈300 cP and 2 mS cm^{-1} at 25 °C [3], and the ionic conductivity of LiTFSI/PP13-TFSI (PP13 = *N*-methyl-*N*-propylpipelidinium, [Li]/([Li] + [PP13]) = 0.12) is 0.51 mS cm^{-1} at 25 °C [4]. Although the temperatures are different, the Li20–K10–Cs70 melt is less viscous and much more ionically conductive than the reported RTILs at each operation temperature.

A cyclic voltammogram of a nickel plate electrode in the Li20–K10–Cs70 melt at 150 °C is shown in Fig. 4. A pair of cathodic and anodic waves is observed at 0 V vs. Li/Li^+, which interpreted as the deposition/dissolution of lithium metal. To confirm this, galvanostatic electrolysis was conducted using a nickel plate electrode at −5 mA for 15 h. Fig. 5 shows an XRD spectrum of the deposit. The obtained peaks are all ascribed to those of lithium metal and CsTFSI. The peaks for LiTFSI and KTFSI are not clearly observed probably due to the lower contents and smaller X-ray scattering coefficients. The deposit was also analyzed by DSC. As shown in Fig. 6, a large endothermic peak arises from 117 °C, corresponding to the eutectic point of the melt. A peak shoulder appearing at higher temperature side indicates a continuous melting of the remaining solid salts that ends by the return to the baseline at 146 °C (mp of Li20–K10–Cs70). Then, a clear endothermic peak starts at 181 °C, which corresponds to the melting of lithium metal. No peaks are observed at melting points of cesium (28 °C) and potassium (63 °C). These results confirm that the reaction at the cathode limit is the deposition of lithium metal. In order to investigate the anode limit of the melt, a cyclic voltammogram was recorded using a glassy carbon rod electrode. As shown in Fig. 7, a sharp increase of anodic current is observed from 5.0 V. Since no cathodic current is observed after the reversal of the scanning direction, the anodic current is believed to correspond to the irreversible oxidation of TFSI anion. Summarizing the voltammetric results of Figs. 4 and 7, the electrochemical window of the melt is determined to be 5.0 V at 150 °C. These results

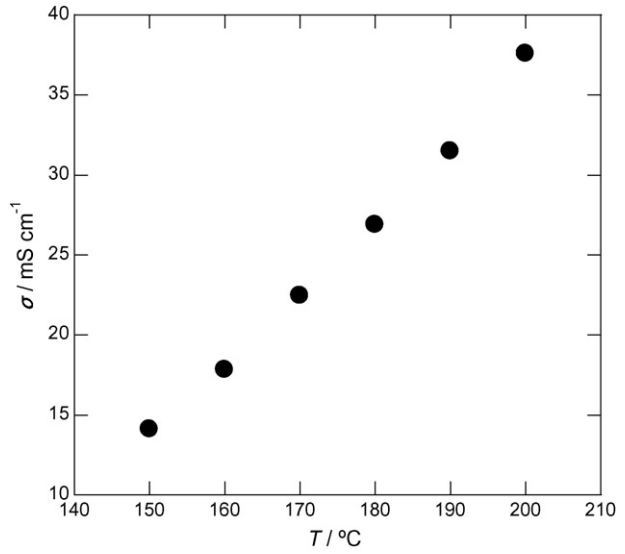

Fig. 3. Temperature dependence of ionic conductivities for Li20–K10–Cs70 melt.

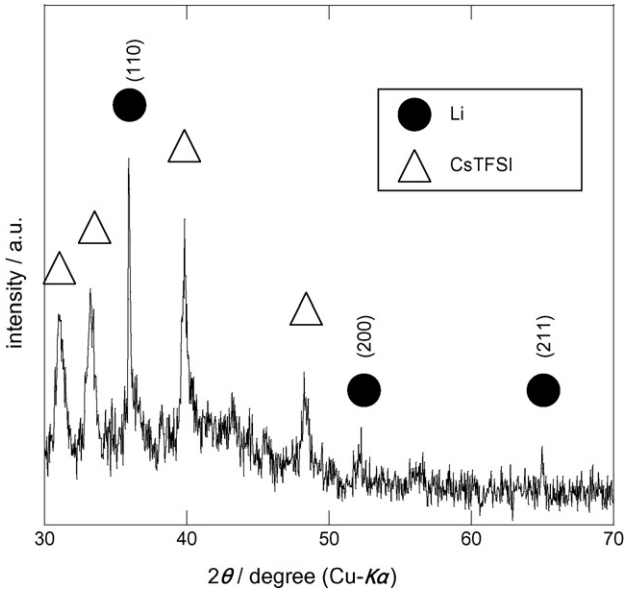

Fig. 5. An XRD spectrum of the deposit obtained by galvanostatic electrolysis for 15 h at −5.0 mA in Li20–K10–Cs70 melt.

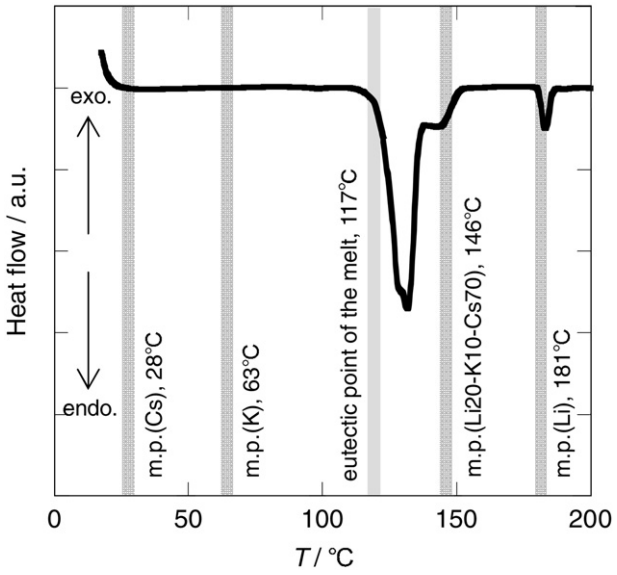

Fig. 6. A DSC curve of the deposit obtained by galvanostatic electrolysis for 15 h at −5.0 mA in Li20–K10–Cs70 melt.

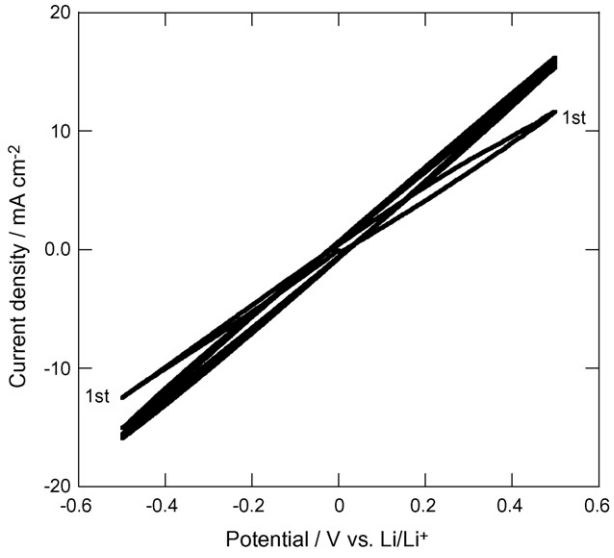

Fig. 8. Cyclic voltammograms of a Li foil electrode in Li20–K10–Cs70 melt at 150 °C for 1st, 100th, 200th, 300th and 400th cycles. Scan rate: 10 mV s^{-1}.

indicate that the Li20–K10–Cs70 melt exhibits excellent properties as an electrolyte for rechargeable lithium batteries at intermediate temperature.

To study the reversibility of lithium deposition/dissolution, cyclic voltammograms were continuously measured for 400 cycles between −0.5 V and 0.5 V using a lithium foil electrode. Fig. 8 shows the obtained voltammograms for the 1st, 100th, 200th, 300th and 400th cycles. Although the current density of the 1st cycle is slightly smaller, the other voltammograms almost overlap, suggesting a fairly good reversibility of the deposition/dissolution of lithium metal in this melt. The cumulative cycling capacity during the 400 cycles is calculated to be ∼84 mA h cm^{-2} that is comparable to the initial lithium electrode capacity (∼100 mA h cm^{-2}). The test with a larger cycle number is now under way to estimate the reversibility of lithium electrode in this melt more precisely.

The stability of aluminum, which was used as a current collector of the cathode, was checked by two methods. Firstly, a current transition was measured during potentiostatic electrolysis of an aluminum plate electrode at 4.5 V. As shown in Fig. 9, no current except noise is observed. Although a severe corrosion of Al has been reported in the organic electrolyte containing LiTFSI under anodic polarization conditions [13,14], such corrosion does not take place in this melt. It is worth noting that the aluminum corrosion also does not occur in a room-temperature LiTFSI/EMI–TFSI electrolyte [3,15]. Secondly, as a more practical test, cyclic voltammetry was conducted for an aluminum mesh electrode, which was used as an actual current collector, in the potential range of 2.0–6.0 V. Fig. 10 shows the measured voltammograms for the 1st, 2nd and 4th cycles. The currents become smaller as the cycle proceeds and are negligibly small in the potential range of 2.8–4.0 V where the following charge–discharge tests were conducted. The surface of the mesh was partly discolored after the experiments. The above results are explained by the formation of passivation film inferred in the previous study [15]. The passivation film is probably formed by a

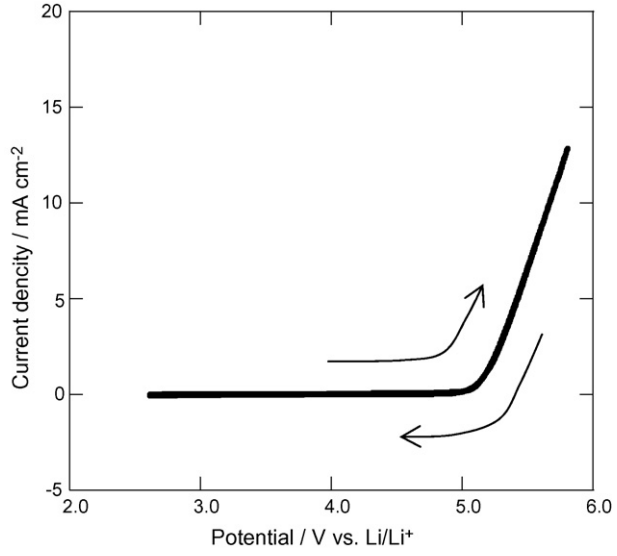

Fig. 7. A cyclic voltammogram of a glassy carbon rod electrode in Li20–K10–Cs70 melt at 150 °C. Scan rate: 10 mV s^{-1}.

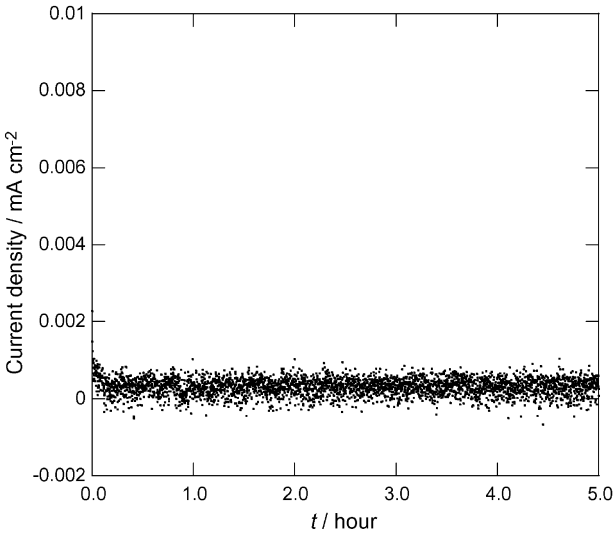

Fig. 9. A chronoamperogram of an aluminum plate electrode in Li20–K10–Cs70 melt at 4.5 V vs. Li/Li$^+$ at 150 °C.

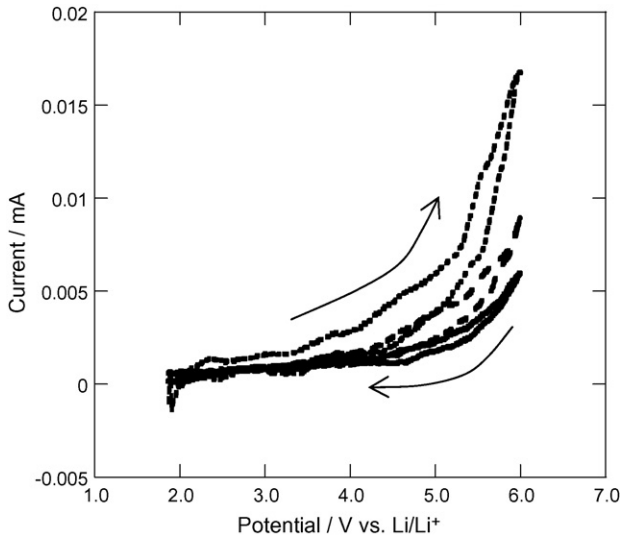

Fig. 10. Cyclic voltammograms of an aluminum mesh electrode in Li20–K10–Cs70 melt at 150 °C for 1st cycle (dotted line), 2nd cycle (dashed line) and 4th cycle (solid line). Scan rate: 1 mV s^{-1}.

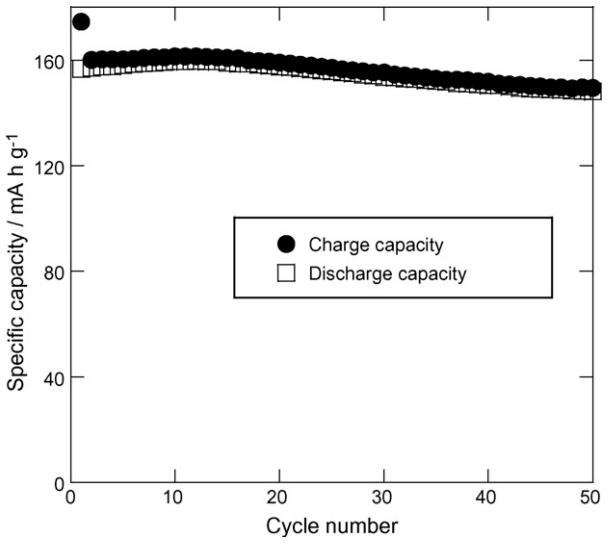

Fig. 12. Cycling properties of the Li/(Li, K, Cs)TFSI/$LiFePO_4$ cell at 150 °C (2.8–4.0 V, constant current at C/10).

reaction of Al^{3+} and $TFSI^-$. The higher current observed in the case of aluminum mesh electrode in the initial cycle shown in Fig. 10 compared to that found in the plate electrode shown in Fig. 9 is probably due to the difference in the active surface area. With the increase of cycling number of the mesh electrode, the current observed at 4.5 V is decreased to the same level that is found for the plate electrode, which is ascribed to the growth of passivation film on the surface of aluminum mesh electrode. For the moment, it is confirmed that Al mesh is practically stable as a current collector of the cathode in the present study.

In this study, $LiFePO_4$, first proposed by Goodenough and his co-workers in 1997 [16], was selected as the cathode active material taking account its high thermal stability at elevated temperatures [17,18]. Carbon coating is necessary to improve the electronic conductivity of $LiFePO_4$. The amount of the coated carbon is estimated to be less than 1 wt% of $LiFePO_4$ in the present study. Charge–discharge tests were performed for the Li/Li20–K10–Cs70 melt/$LiFePO_4$ cell at a constant current rate of C/10 between 2.8 V and 4.0 V for 50 cycles at 150 °C. As shown in Fig. 11, flat potential plateaus were repeatedly observed at approximately 3.4 V in both charge and discharge curves. The specific capacities reach 145–160 mA h g^{-1}. The value 160 mA h g^{-1} corresponds to 94% in the utility of active mass. Fig. 12 shows the cycling properties during the charge–discharge tests. During the initial few cycles except for the first charge, both the charge and discharge capacities gradually increase and then decrease. After 40 cycles, specific capacities become almost constant and approximately 95% of the initial discharge capacity is maintained after 50 cycles, indicating the high stabilities of the melt and all the electrode materials at 150 °C. The coulombic efficiencies during these 50 cycles are plotted in Fig. 13. Except for the 1st cycle, the coulombic efficiencies are almost 100% for all the cycles. From the above results, it is concluded that the Li/Li20–K10–Cs70 melt/$LiFePO_4$ cell is highly promising as

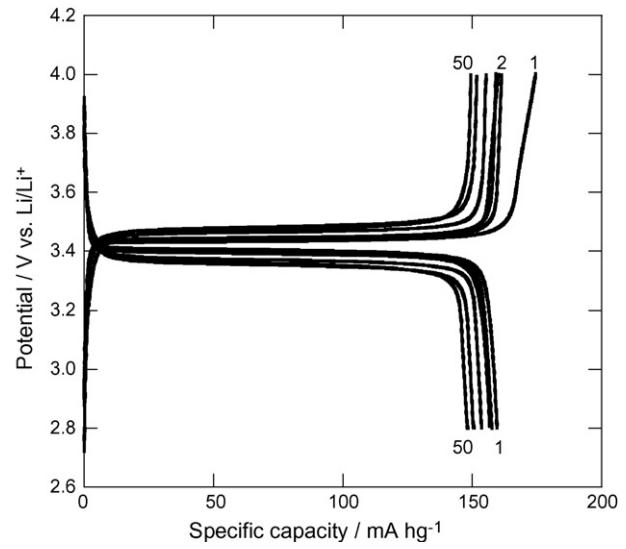

Fig. 11. Charge–discharge curves of the Li/Li20–K10–Cs70 melt/$LiFePO_4$ cell for 1st, 2nd, 10th, 20th, 30th, 40th and 50th cycles at 150 °C (2.8–4.0 V, constant current at C/10).

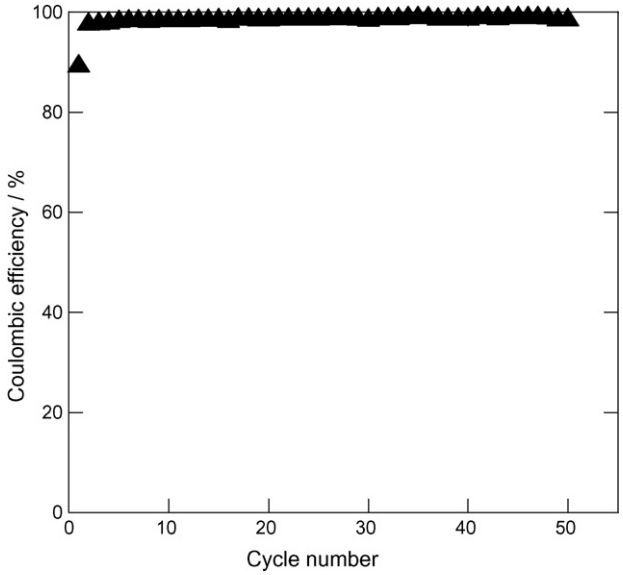

Fig. 13. Coulombic efficiencies for charge and discharge during 50 cycles of the Li/(Li, K, Cs)TFSI/$LiFePO_4$ cell at 150 °C (2.8–4.0 V, constant current at C/10).

a new rechargeable lithium metal battery operating at intermediate temperature.

4. Conclusion

The (Li, K, Cs)TFSI (Li20–K10–Cs70) melt is less viscous and more ionically conductive than RTILs in which LiTFSI is dissolved at respective operation temperatures. The electrochemical window of the Li20–K10–Cs70 melt is 5.0 V at 150 °C and the cathode limit reaction of this melt is the deposition of lithium metal. An aluminum is a stable material as a current collector of the cathode in this melt. The Li/Li20–K10–Cs70 melt/$LiFePO_4$ cell showed an excellent cycle performance at 150 °C and 95% of the initial discharge capacity is maintained after 50 cycles with coulombic efficiencies of almost 100%. It is concluded that the Li20–K10–Cs70 melt is a promising electrolyte for rechargeable lithium battery at elevated temperatures, and that $LiFePO_4$ is a stable cathode material under the charge–discharge cycles even at 150 °C.

Acknowledgement

This work was financially supported by a Grant in Aid for Scientific Research for Priority Area “Science of Ionic Liquids” from the Japanese Ministry of Education, Culture, Sports, Science, and Technology.

References

[1] M. Broussely, Fr. Poitiers, in: G.-A. Nazri, G. Pistoia (Eds.), Lithium Batteries: Science and Technology, Kluwer Academic Publishers, 2004, pp. 645–685.
[2] M. Majima, S. Ujiie, E. Yagasaki, S. Inazawa, K. Miyazaki, J. Power Sources 92 (2001) 108–119.
[3] B. Garcia, S. Lavallée, G. Perron, C. Michot, M. Armand, Electrochim. Acta 49 (2004) 4583–4588.
[4] H. Sakaebe, H. Matsumoto, Electrochem. Commun. 5 (2003) 594–598.
[5] F. Croce, G.B. Appetecchi, L. Persi, B. Scrosati, Nature 394 (1998) 456–458.
[6] I. Galasiu, R. Galasiu, J. Thonstad, in: D. Aurbach (Ed.), Nonaqueous Electrochemistry, Marcel Dekker, New York, 1999, pp. 461–591.
[7] Y. Ito, T. Nohira, Electrochim. Acta 45 (2000) 2611–2622.
[8] H. Ohno (Ed.), Electrochemical Aspects of Ionic Liquids, John Wiley & Sons Inc., New York, 2005.
[9] R. Hagiwara, K. Tamaki, K. Kubota, T. Goto, T. Nohira, J. Chem. Eng. Data 53 (2008) 355–358.
[10] K. Kubota, T. Nohira, T. Goto, R. Hagiwara, J. Chem. Eng. Data, submitted for publication.
[11] T. Nohira, T. Goto, R. Hagiwara, Yoyuen oyobi Koon Kagaku 51 (2008) 148–154.
[12] J.-M. Kim, K. Ohtsuki, K. Abiko, Y. Kadoma, K. Ui, N. Kumagai, Abstract volume of the 212th Electrochemical Society Meeting, 2007, p. 639.
[13] M. Morita, T. Shibata, N. Yoshimoto, M. Ishikawa, Electrochim. Acta 47 (2002) 2787–2793.
[14] M. Morita, T. Shibata, N. Yoshimoto, M. Ishikawa, J. Power Sources 119-121 (2003) 784–788.
[15] B. Garcia, M. Armand, J. Power Sources 132 (2004) 206–208.
[16] A.K. Padhi, K.S. Nanjundaswamy, J.B. Goodenough, J. Electrochem. Soc. 144 (1997) 1188–1194.
[17] Z. Bakenov, M. Nakayama, M. Wakihara, Electrochem. Solid-State Lett. 10 (2007) A208–A211.
[18] M. Takahashi, S. Tobishima, K. Takei, Y. Sakurai, Solid State Ionics 148 (2002) 283–289.